



Title:

Topology Optimization Method for Multi-Patch FDM Printing Based on Dynamic Loads and Anisotropic Characteristics

Authors:

Kaiyuan Meng, ky.meng@mail.sdu.edu.cn, Shandong University
Jikai Liu, jikai_liu@sdu.edu.cn, Shandong University

Keywords:

Topology Optimization, FDM, Dynamic Structure, Material Anisotropy

DOI: 10.14733/cadconfP.2025.198-204

Introduction:

Additive manufacturing (AM) technology, with its manufacturing method of depositing materials layer by layer, can realize the processing of complex geometric shapes, breaking the limitations of traditional manufacturing processes, providing greater freedom for performance-oriented design, and effectively avoiding manufacturability issues [1]. Design for Additive Manufacturing (DfAM) aims to generate geometries that meet manufacturing requirements and optimize performance [2]. As a powerful design method, topology optimization (TO) has gradually become an ideal choice in this field because it can give full play to the flexibility of DfAM [3]. In recent years, more and more studies have incorporated the constraints inherent in additive manufacturing into the topology optimization framework, such as limiting the overhang angle and controlling the size scale of design features [4,5]. These innovations have provided new development directions for topology optimization in AM and promoted the application and advancement of this method [6].

Since AM adopts a layer-by-layer manufacturing method, almost all AM materials exhibit varying degrees of anisotropic characteristics [7], and this phenomenon is particularly obvious in fused deposition modeling (FDM). In fact, fully considering the anisotropic properties of materials in topology optimization can effectively narrow the performance gap between the designed structure and the actual manufactured structure.

Taking fiber composite 3D printing as an example, the initial research idea is to use fiber angle as a complementary variable field to achieve collaborative design of structural topology optimization and fiber deposition direction optimization. However, due to the disordered nature of fiber orientations, the resulting designs were often difficult to directly apply to manufacturing [8]. In order to solve this problem, Lee et al. [9] proposed a method to discretize the topology into unidirectionally deposited components to achieve segmented continuous fiber orientation optimization to reduce the complexity of the fiber orientation field. Subsequently, Papapetrou et al. [10] further post-processed the optimized fiber orientation and proposed a variety of fiber deposition modes, including contour offset mode, streamline mode etc., to improve the implement ability of the deposition path.

However, in practical applications, most FDM machines only support the hybrid deposition path (HDP) mode, which achieves material deposition by filling the internal structure after the contour offset in a zigzag shape. Therefore, for this mode, Liu et al. [11] proposed a level set-based method that combines hybrid deposition path planning with shape optimization and topology optimization to improve the performance of the printed structure. In addition, Xu et al. [12] used the SIMP method to carry out topology optimization research based on HDP, fully considering the influence of material

anisotropy in the topological structure formation process. Meng et al. [13] further expanded this method to the dynamic level, studying the dynamic response of the structure under various excitation conditions, and verified it through numerical calculations and experiments.

Notably, existing studies on co-optimization of printing directions and topology in HDP mode rarely address multiple orientations. Forcing a uniform direction across all substrate domains is often inefficient, as varying directions in specific regions can enhance performance [14]. Therefore, we propose a multi-patch design framework that divides the substrate into regions with distinct orientations, improving overall performance. Fig. 1 illustrates this framework in HDP mode. Using an enhanced double smoothing projection (DSP) filter to separate the contour offset layer, material properties are modeled via coordinate transformation of an orthotropic constitutive model [12,13].

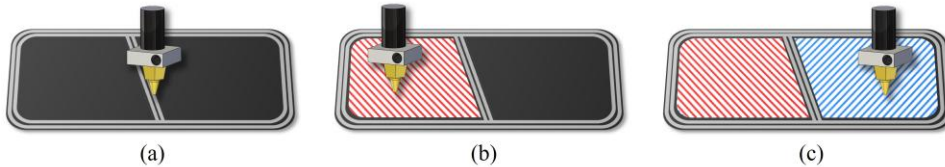


Fig. 1: Illustration of the multi-patch HDP pattern (a) Print the boundary layer (b) Print the substrate domain with direction #1 (c) Print the substrate domain with direction #2.

In summary, this study addresses the concurrent optimization of orientation and density distribution under dynamic loads and material anisotropy in HDP mode. We introduce an improved DSP filter and SOMP (solid orthotropic material with penalty) interpolation method for concurrent topology and direction optimization. The extended-SIMP method couples substrate materials across directions, effectively modeling material anisotropy and generating optimal structures and manufacturing solutions for dynamic environments. The main contributions are as follows:

- *Orientation-density distribution collaborative optimization method*: A novel multi-patch design framework for concurrent optimization of topology and printing direction under dynamic loads and material anisotropy.
- *Full-scale material anisotropy modeling and dynamic environment optimal structure generation*: Efficient material anisotropy modeling and optimal structure generation through precise contour offset separation and refined density distribution in the substrate domain.

Optimization problem formulation:

The time-discrete form of the equation of the $ndof$ -freedom discrete structure under simple harmonic load can be expressed as:

$$\mathbf{M}\ddot{\mathbf{u}} + \mathbf{C}\dot{\mathbf{u}} + \mathbf{K}\mathbf{u} = \mathbf{p} \quad (2.1)$$

Where \mathbf{p} represents the time-dependent dynamic load, expressed as $\mathbf{p}(t) = \mathbf{P}e^{i\omega_p t}$, with amplitude \mathbf{P} and frequency ω_p . \mathbf{u} represents the displacement vector, where the amplitude of the displacement can be written as \mathbf{U} , $\dot{\mathbf{u}}$ and $\ddot{\mathbf{u}}$ represent the first and second order time derivatives of the displacement, i.e., velocity and acceleration, respectively. Therefore, Eqn. (2.1) can be rewritten as:

$$(-i\omega_p^2 \mathbf{M} + i\omega_p \mathbf{C} + \mathbf{K})\mathbf{U} = \mathbf{P} \quad (2.2)$$

$$\mathbf{K}_d = (-i\omega_p^2 \mathbf{M} + i\omega_p \mathbf{C} + \mathbf{K}) \quad (2.3)$$

Here \mathbf{K}_d represents the dynamic stiffness matrix. In addition, since the influence of damping is not considered in this paper, \mathbf{C} is ignored in the subsequent analysis. According to the classical laminate theory, the directional elastic tensor of anisotropic materials can be expressed in the form of Eqn. (2.4) [12].

$$\mathbf{D}(\theta) = \mathbf{T}(\theta)\mathbf{D}_0\mathbf{T}(\theta)^T \quad (2.4)$$

Where \mathbf{D}_0 is the unrotated elastic tensor and \mathbf{T} is the coordinate transformation matrix [13]. Next, we differentiate the design domain based on the improved DSP method to obtain the substrate domain and boundary layer. The algorithm consists of two main parts, namely, PDE filter and the Heaviside projection [15]. Their equation is as follows:

$$-r^2 \nabla^2 \tilde{x} + \tilde{x} = x \quad \mu = \frac{\tanh(\beta\eta) + \tanh(\beta(\tilde{x} - \eta))}{\tanh(\beta\eta) + \tanh(\beta(1 - \eta))} \quad (2.5)$$

Where x is the initial design variable, \tilde{x} is a smoothing variable. r is a length scale parameter, which has a numerical relationship with the classical filter radius R . Then the smoothed variables were truncated using Heaviside projection. β here represents the sharpness of the Heaviside function, and the threshold η is 0.95. And the boundary thickness w can be precisely controlled by the filter radius R [15].

Fig. 2 shows a flow chart of separating the substrate domain from the boundary layer when only one substrate domain filling direction is predefined. The design variable x_1 is filtered by DSP to obtain the corresponding substrate domain τ_1 and boundary layer χ_b^1 . At the same time, we can assign the predefined direction θ_s to the substrate domain τ_1 and obtain the boundary layer direction field θ_b through the spatial gradient of the intermediate density field $\tilde{\mu}_1$, and finally get the distribution of all directions in the design domain.

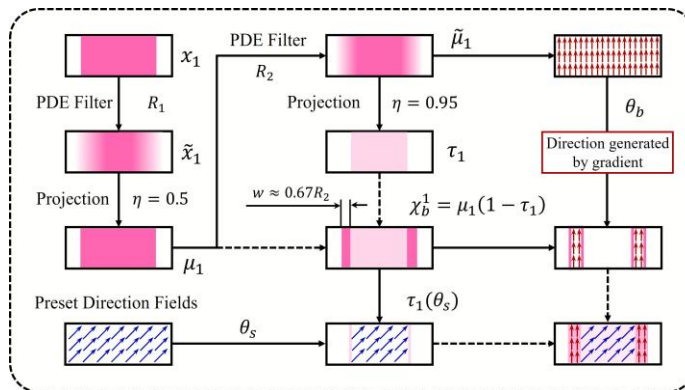


Fig. 2: Schematic diagram of the process of dividing the design domain into the substrate domain and the boundary layer through DSP and obtaining the corresponding directions.

Since the directions between the substrate domain and the boundary layer are different, based on the SOMP model the elastic tension and density of the entire structure can be expressed as:

$$D^1(x_1) = D_s \tau_1^p + D_b \mu_1^p (1 - \tau_1^p) \quad \rho^1(x_1) = \rho_s \tau_1 + \rho_b \mu_1 (1 - \tau_1) \quad (2.6)$$

D_s and D_b in Eqn. (2.6) represent the elastic tension of the substrate domain and boundary layer respectively, which are related to the directions θ_s and θ_b . p represents the penalty factor. Based on the extended-SIMP interpolation, we can treat the substrate domains at different directions as different materials for analysis. When there are N filling directions in the substrate domain, the elastic tension D^N and density interpolation ρ^N of the entire structure can be expressed as follows:

$$D^N(x_1, x_2, \dots, x_N) = \sum_{i=1}^N D_s^i \Xi_i^s + D_b^i \Xi_i^b \quad \rho^N(x_1, x_2, \dots, x_N) = \sum_{i=1}^N \rho(\psi_i^s + \psi_i^b) \quad (2.7)$$

where D_s^i and D_b^i represent the elastic tension of the substrate domain and boundary layer corresponding to the i -th direction. The $\Xi_i^s, \Xi_i^b, \psi_i^s, \psi_i^b$ are equations of the design variable $x_i (i = 1 : N)$, which can be written as follows:

$$\Xi_i^s = (1 - \tau_{i-1}^p)(1 - \mu_{i-1}^p) \prod_{j=i}^N \tau_j^p \quad \Xi_i^b = \sum_{i=1}^N \left[(1 - \tau_i^p) \mu_i^p \prod_{j=i+1}^N \tau_j^p \right] \quad (2.8)$$

$$\psi_i^s = (1 - \tau_{i-1})(1 - \mu_{i-1}) \prod_{j=i}^N \tau_j \quad \psi_i^b = \sum_{i=1}^N \left[(1 - \tau_i) \mu_i \prod_{j=i+1}^N \tau_j \right] \quad (2.9)$$

We take the case that there are two directions θ_s^1 and θ_s^2 in the substrate domain ($N=2$) as an example, the structural model is shown in Fig. 3.

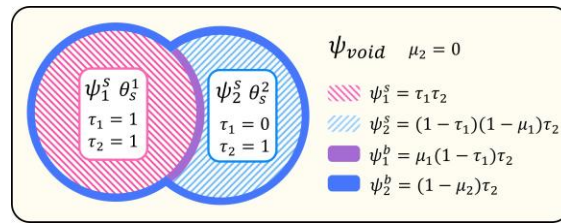


Fig. 3 Simple schematic diagram of the substrate domain and boundary layer at multiple directions.

It is worth noting that the direction of the boundary layer is calculated based on the gradient. Therefore, its elastic tension is quite different and essentially based on the derivative of the design variable. For example, in this case, there are two boundary layers ψ_1^b and ψ_2^b , and their corresponding directions can be expressed by the following equation:

$$\theta_b^1 = \frac{\pi}{2} + \arctan\left(\frac{\partial \tilde{\mu}_1}{\partial y} / \frac{\partial \tilde{\mu}_1}{\partial x}\right) \quad \theta_b^2 = \frac{\pi}{2} + \arctan\left(\frac{\partial \tilde{\mu}_2}{\partial y} / \frac{\partial \tilde{\mu}_2}{\partial x}\right) \quad (2.10)$$

Based on all the above preparations, combined with Eqn. (2.2), we take minimizing the overall vibration response under a fixed excitation load as the optimization goal, that is, minimizing the norm of the dynamic compliance of the structure [16].

$$\begin{aligned} & \text{find} : x_i (i = 1, \dots, N), \theta_s^i (i = 1, \dots, N) \\ & \text{min} : Cd = \|\mathbf{P}^T \mathbf{U}\| \\ & \text{s.t.} : \begin{cases} \mathbf{K}_d \mathbf{U} = (\mathbf{K} - \omega_p^2 \mathbf{M}) \mathbf{U} = \mathbf{P} \\ G_i = V_i / \bar{V} - f_i \leq 0, (i = 1, \dots, N) \\ x_e \in [10^{-3}, 1], \theta_e \in [-2\pi, 2\pi] \end{cases} \end{aligned} \quad (2.11)$$

In the formula, G_i represents the volume constraint, f_i is the proportion of the substrate domain in each direction, and V_i is the volume calculation formula of the i -th substrate, as shown below:

$$V_i = \sum_{k=1}^{nele} \left[1 - \mu_{i-1} \prod_{j=i}^N \mu_j \right] \quad (2.12)$$

Where $nele$ represents the total number of elements corresponding to the finite element mesh.

Numerical Example:

In this section, we will use a half-simply supported beam case to demonstrate the effectiveness of our optimization algorithm. As shown in Fig. 4, in order to better demonstrate the boundary layer effect, a non-design domain is set around its edge. The structure is discretized into 160*160 units, and the

material parameters are set as shown in the following table. The load is 200kN with an amplitude P and a frequency of 100Hz. The initial directions are set to 0° and 90° , respectively. The volume fraction of the two directions is 0.25. The optimization iteration process is shown in Fig. 5.

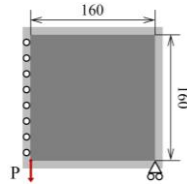


Fig. 4: Design domain of optimized structure.

Material parameters	Young's modulus in x direction	Young's modulus in y direction	Poisson's ratio in the xy direction	Density	Filter radius of density field x_1	Filter radius of density field x_2	Boundary layer thickness
Numeric	$E_x = 50\text{GPa}$	$E_y = 25\text{GPa}$	$\nu_{xy} = 0.4$	$\rho = 1\text{kg/m}^3$	$R_1 = 6$	$R_2 = 6$	$w = 2$

Tab. 1: Material parameters used in the optimization.

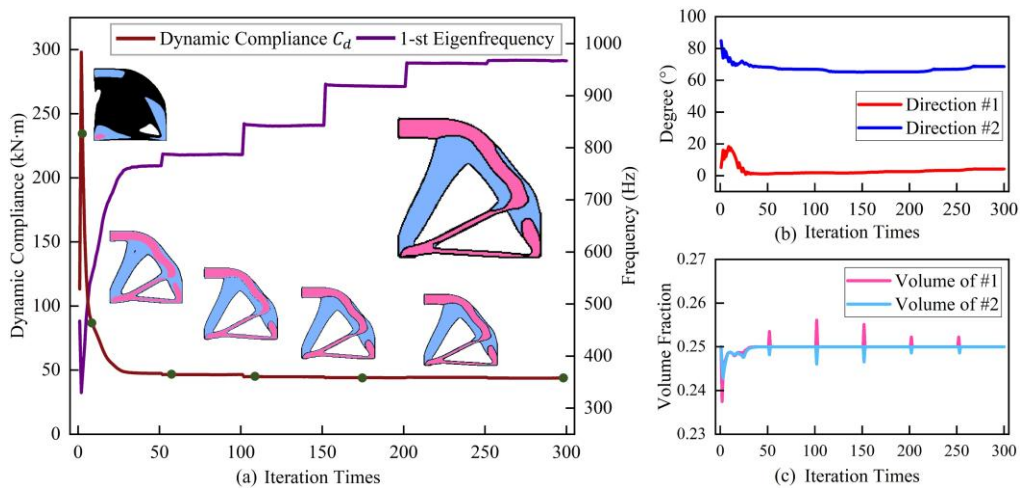


Fig. 5: The optimization process (a) Iterative process of structural dynamic compliance and 1-st eigenfrequency (b) Iterative process of directions of substrate domain (c) Iterative process of volume fraction corresponding to two directions.

Combined with Fig. 5, it is not difficult to see that the iteration converges smoothly, and all parameters have been optimized to a certain extent. The dynamic compliance is reduced from 113.25kN·m to 43.85kN·m, and the first eigenfrequency is increased to 967Hz. The two directions finally optimized are 4.21° and 68.23° , respectively. In Fig. 6, we also show the directional details of the two base domains and the two boundary layers.

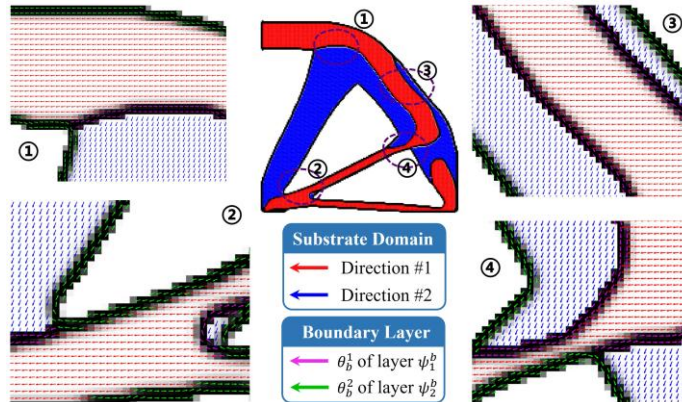


Fig. 6: Schematic diagram of printing direction of each area.

Conclusions:

This paper proposes a multi-patch dynamic topology optimization method for the anisotropic properties of materials in the HDP mode. Based on the erosion DSP algorithm and the extended SIMP interpolation model, a material interpolation model suitable for multi-patch conditions is constructed. The optimization results show that this method can effectively realize regional division and optimization, significantly improve the dynamic performance of the structure, and reduce material consumption, providing a theoretical basis and technical support for multi-patch FDM printing.

References:

- [1] Liu, J.; Ma, Y.: A survey of manufacturing-oriented topology optimization methods, *Advances in Engineering Software*, 2016, 100, 161–75. <https://doi.org/10.1016/j.advengsoft.2016.07.017>
- [2] Xu, S.; Liu, J.; Sun, Y.; Li, X.; Ma, Y.: Support structure topology optimization considering the residual distortion for laser powder bed fusion metal additive manufacturing, *Struct Multidisc Optim*, 2024, 67, 182. <https://doi.org/10.1007/s00158-024-03883-y>
- [3] Xu, S.; Liu, J.; Yaji, K.; Lu, L.: Topology optimization for hybrid additive-subtractive manufacturing incorporating dynamic process planning, *Computer Methods in Applied Mechanics and Engineering*, 2024, 431, 117270. <https://doi.org/10.1016/j.cma.2024.117270>
- [4] Guo, Y.; Liu, J.; Ahmad, R.; Ma, Y.: Concurrent structural topology and fabrication sequence optimization for multi-axis additive manufacturing, *Computer Methods in Applied Mechanics and Engineering*, 2025, 435, 117627. <https://doi.org/10.1016/j.cma.2024.117627>
- [5] Liu, J.; Zhang, C.; Zou, B.; Li, L.; Yu, H.: Topology optimisation for vat photopolymerization 3D printing of ceramics with flushing jet accessibility constraint, *Virtual and Physical Prototyping*, 2024. <https://doi.org/10.1080/17452759.2024.2303717>
- [6] Liu, S.; Li, Q.; Hu, J.; Chen, W.; Zhang, Y.; Luo, Y.; et al.: A Survey of Topology Optimization Methods Considering Manufacturable Structural Feature Constraints for Additive Manufacturing Structures, *Additive Manufacturing Frontiers*, 2024, 3, 200143. <https://doi.org/10.1016/j.amf.2024.200143>
- [7] Zhang, P.; Liu, J.; To, A.C.: Role of anisotropic properties on topology optimization of additive manufactured load bearing structures, *Scripta Materialia*, 2017, 135, 148–52. <https://doi.org/10.1016/j.scriptamat.2016.10.021>
- [8] Xia, Q.; Shi, T.: Optimization of composite structures with continuous spatial variation of fiber angle through Shepard interpolation, *Composite Structures*, 2017, 182, 273–82. <https://doi.org/10.1016/j.compstruct.2017.09.052>
- [9] Lee, J.; Kim, D.; Nomura, T.; Dede, E. M.; Yoo, J.: Topology optimization for continuous and discrete orientation design of functionally graded fiber-reinforced composite structures, *Composite Structures*, 2018, 201, 217–33. <https://doi.org/10.1016/j.compstruct.2018.06.020>

- [10] Papapetrou, V. S.; Patel, C.; Tamijani, A.Y.: Stiffness-based optimization framework for the topology and fiber paths of continuous fiber composites, *Composites Part B: Engineering*, 2020, 183, 107681. <https://doi.org/10.1016/j.compositesb.2019.107681>
- [11] Liu, J.; Ma, Y.; Qureshi, A. J.; Ahmad, R.: Light-weight shape and topology optimization with hybrid deposition path planning for FDM parts, *Int J Adv Manuf Technol*, 2018, 97, 1123-35. <https://doi.org/10.1007/s00170-018-1955-4>
- [12] Xu, S.; Huang, J.; Liu, J.; Ma, Y.: Topology Optimization for FDM Parts Considering the Hybrid Deposition Path Pattern, *Micromachines*, 2020, 11, 709. <https://doi.org/10.3390/mi11080709>
- [13] Meng, K.; Fu, J.; Qu, D.; Li, L.; Liu, J.: Dynamic topology optimization incorporating the material anisotropy feature for 3D printed fiber composite structures, *Finite Elements in Analysis and Design*, 2025, 243, 104281. <https://doi.org/10.1016/j.finel.2024.104281>
- [14] Jiang, D.; Hoglund, R.; Smith, D. E.: Continuous Fiber Angle Topology Optimization for Polymer Composite Deposition Additive Manufacturing Applications, *Fibers*, 2019, 7:14. <https://doi.org/10.3390/fib7020014>
- [15] Luo, Y.; Li, Q.; Liu, S.: Topology optimization of shell-infill structures using an erosion-based interface identification method, *Computer Methods in Applied Mechanics and Engineering*, 2019, 355, 94-112. <https://doi.org/10.1016/j.cma.2019.05.017>
- [16] Du, J.; Olhoff, N.: Minimization of sound radiation from vibrating bi-material structures using topology optimization, *Struct Multidisc Optim*, 2007, 33, 305-21. <https://doi.org/10.1007/s00158-006-0088-9>